

On instationary mechanisms in cavitating micro throttles

B Beban¹, S Legat¹, S J Schmidt¹ and N A Adams¹

¹ Technische Universität München, Institute of Aerodynamics and Fluid Mechanics,
D-85746 Garching, Germany

E-mail: bruno.beban@tum.de

Abstract. The current investigation presents numerical simulations of cavitating flows in a simplified model of a mushroom valve chamber of a piezo common rail injection system. Two discharge throttles with different step diameters are investigated. The developed models are able to predict relevant features of cavitating flow in fuel injectors. Special attention is put on the investigation of wave dynamics and related instationary mechanisms in the discharge throttle and the valve chamber. To this respect, a compressible flow solver with a homogeneous mixture model and barotropic description of the diesel-like-fluid is utilized. Highly unsteady phenomena are observed in both investigated designs. The structure of the cavitating flow is further analyzed with an emphasis on the interaction between collapsing vapor clouds in the throttle step and reentrant motion in the discharge throttle. Furthermore, numerical simulations reveal significant influence of the throttle step diameter on the cavity dynamics.

1. Introduction

Modern common rail injection systems exceed injection pressures of more than 2000 bar, with the aim to improve fuel injection efficiency and to meet demanding emission standards. However, huge pressure drops through the throttles cause the working fluid to cavitate. For the valve chamber, which regulates fuel injection sequencing, cavitating throttles in choked regime are used to ensure constant and pressure-drop independent mass flow rates. Formation of the instantaneous pressure peaks due to the collapse of cavitating clouds, accompanied by the high loads on the material surface, may therefore cause a failure of system components.

In this study, we investigate the cavitating flow in the valve chamber of a piezo common rail injection system. Since a realistic, three-dimensional model of the chamber – which consists of the discharge throttle, mushroom valve, return spring, valve piston and outlet passage – is expensive from the computational viewpoint, a simplified model is developed. It enables a detailed investigation of the complex flow physics at reduced geometrical complexity. Experimental investigation of micro channels is usually limited to planar geometries [1, 2, 3], or large-scaled orifices [4], since they are accessible by optical measurement techniques. Recent x-ray radiography measurements show promising results of averaged vapor volume prediction in axis-symmetric micro channels [5]. However, experimental measurements of highly instationary cavitating flows in micro channels still represent a challenge and hence numerical simulation can provide valuable information about the flow dynamics of small scale structures.



2. Numerical method

For the numerical simulations, we apply our in-house code CATUM (**C**avitation **T**echnische **U**niversität **M**ünchen), which is a finite volume, density-based compressible flow solver. The compressible formulation captures the formation of pressure peaks during the collapse stages of vapor clouds, and consecutive development of shock fronts, which are a driving mechanism for cavitation erosion. Under the assumption that all phases are in thermodynamic equilibrium, phase transition is modeled with a homogeneous mixture approach. We neglect viscosity, since the focus of this study is put on the effects dominated by inertia. Detailed description of the underlying numerics can be found in [6]. The system of governing equations is closed with the barotropic equation of state for diesel-like ISO4113 fluid. Fitting parameters for the equation of state are taken from [7] and [8].

3. Computational grids and numerical setup

The present numerical study includes two different designs of the discharge throttle that connects the high pressure chamber with the valve chamber. The setup, together with an overview of the whole numerical domain, is sketched in Fig. 1. The geometries differ only in the throttle design, keeping the valve chamber and the distance between the throttle outlet and front side of the mushroom valve constant. Both designs feature a cylindrical throttle with length $l = 0.5$ mm, diameter $d = 0.2$ mm and a sharp inlet edge. Designs A and B have step diameters $D_A = 0.5$ mm and $D_B = 1$ mm, respectively. The step length $L = 0.5$ mm is equal for both cases. Block-structured decomposition of the computational domain is utilized. For each design, three grid levels have been created: coarse, medium and fine. The fine grid consists of approximately $2.2 \cdot 10^6$ hexahedral cells. On the fine grid, the discharge throttle is resolved with 49 cells in diameter and 48 along its axis, with a cell size of approximately $4 \mu\text{m}$ across the diameter.

At inlet and outlet, asymptotic boundary conditions for static pressure are prescribed ($p_{in} = 2000$ bar, $p_{out} = 60$ bar). For velocities, von Neumann boundary conditions are imposed. Walls are modelled as adiabatic, inviscid walls.

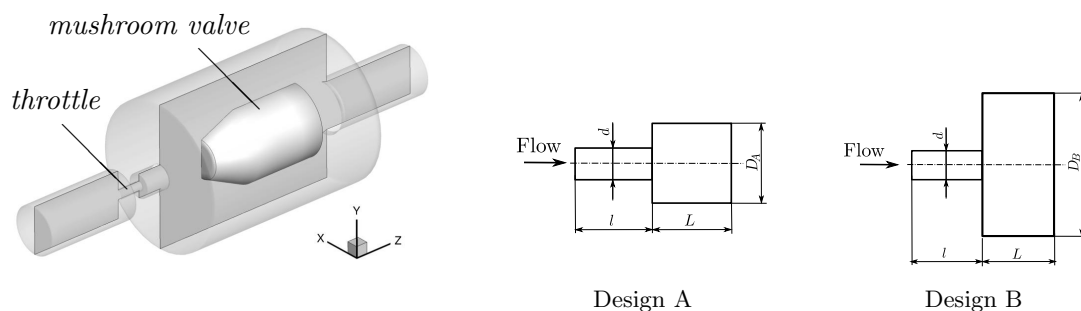


Figure 1. Computational model of the simplified mushroom valve chamber (left) and sketches of the utilized designs (right).

Explicit time discretization of the governing equations results in an order of magnitude $\mathcal{O}(1 \cdot 10^{-10})$ for the time step. Since the time step size is directly proportional to the smallest cell length, a grid sequencing technique is employed to reduce the computational effort: flow field is first established on the coarser grid and successively interpolated onto the finer. In the following, results obtained on the finest grid level are presented.

4. Results and discussion

Design A

A transient behaviour of the cavitating flow in the valve chamber and throttle is observed for design A. Figure 2 depicts a series of six instants in time with a time interval $\Delta t = 1.38 \cdot 10^{-6}$ s

between consecutive pictures. The entire interval t_{1-6} spans $6.4 \cdot 10^{-6}$ s. At the first time instant, a cavitating sheet in the throttle separates from the stable cavity that begins from the throttle entrance. A high speed cavitating jet discharges from the throttle into the valve chamber with velocity of approximately 670 m/s. Low pressure cores in the shear layer around the high speed jet and the surrounding liquid initiate vortex cavitation and form toroidal vapor clouds. Such clouds grow until time instant (2), while the sheet cavity in the throttle continuously sheds further vapor clouds. At time instant (3), a part of the vapor cloud is convected downstream, while the other part remains entrapped by the recirculation eddy that forms within the step. At time instant (4), a supercavitating sheet that spans through the complete throttle is observed. The convected cloud separates and the chamber pressure is imposed on the vapor cloud in the step. This pressure forces the cavitating structure to recondensate and finally to collapse (frames (4)-(6)). Between time instants (5) and (6), the vapor fragment marked by a circle has collapsed, causing a significant pressure rise in the step. At time instant (6), the sheet cavity breaks up near the throttle exit and reduces in length. Once annular shaped vapor structures form in the throttle step, the cycle starts anew.

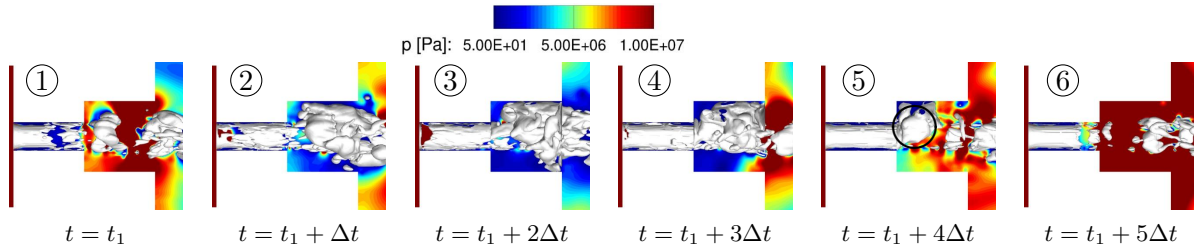


Figure 2. Pressure contours and isosurfaces of vapor volume fraction $\alpha = 0.1$ showing the instationary process in the throttle step. Time interval $t_{1-6} = 6.4 \cdot 10^{-6}$ s.

The onset of reentrant flow is induced before the final collapse stage of the vapor cloud. This leads us to the conclusion that not the shock wave formation after the cloud collapse, but the inertial effect of the collapsing vapor cloud triggers the beginning of the reentrant motion.

Design B

For this configuration, fluid from the chamber discharges into the valve chamber and two counter-rotating eddies form in the step. These vortices interact with the high speed jet. The pressure drop in the shear layer forms toroidal vapor clouds similar to those in design A. However, the highly instationary mechanism that initiates reentrant flow in the throttle differs from that in design A, since no vapor clouds are enforced by the recirculation eddies to stay in the step and to collapse there. Instead, vapor clouds partially collapse at the exit of the throttle step, emitting shock waves that lead to a pressure rise in the step. This mechanism triggers a reentrant motion in the throttle. Figure 3 depicts the process of shock wave propagation in the throttle step at four successive instants in time. The entire time interval t_{1-4} is $4.66 \cdot 10^{-7}$ s long, with $\Delta t = 1.165 \cdot 10^{-7}$ s between each frame. In frame (4), an increase of the pressure in the throttle is clearly visible and can be connected directly to the collapse of the vapor fragments at the throttle exit.

In order to investigate the periodic behaviour of the cavitation flow, we analyse the mass flow at the throttle outlet for both designs, which is depicted in Fig. 4. A periodic drop in mass flow is caused by the reentrant flow at the throttle exit. For design A, frequency spectra reveal one dominant frequency $f_{1A} \approx 135$ kHz, which has also been identified by the visual inspection as the frequency of the collapsing vapor cloud in the throttle step. At least two harmonic modes

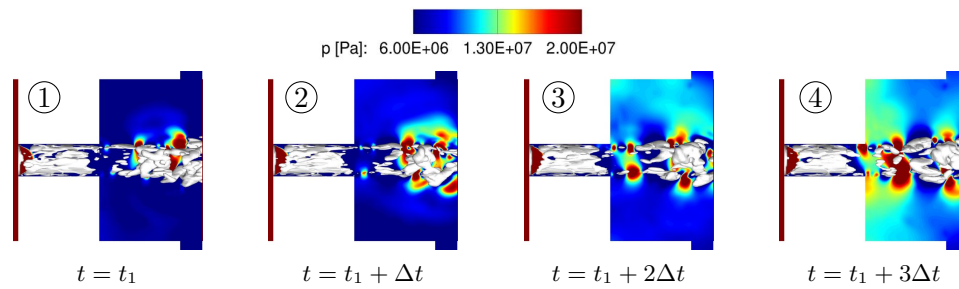


Figure 3. Formation of a shock wave after the collapse of a vapor fragment near the exit of the throttle step, visualized by pressure contours and isosurfaces of vapor volume fraction $\alpha = 0.1$.

are captured by the fast Fourier algorithm. Design B features also one dominant frequency, $f_{1B} \approx 190$ kHz.

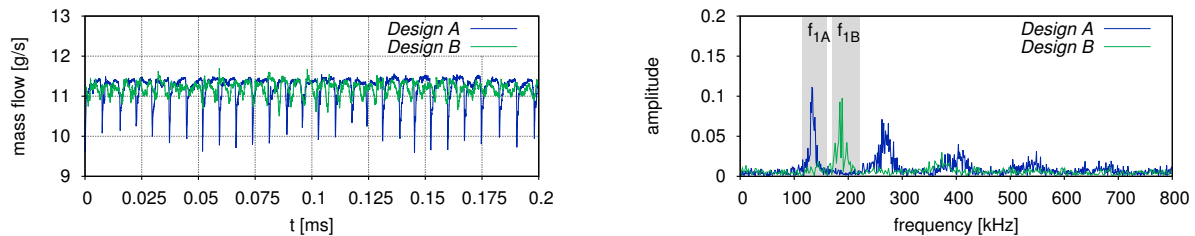


Figure 4. Time history of the mass flow at the exit of the discharge throttle (left); Fast Fourier analysis of the mass flows (right). Dominant frequencies highlighted with f_{1A} and f_{1B} .

We therefore conclude that two different mechanisms triggering the reentrant motion in the discharge throttle have been detected. Owing to the shrinking vapor cloud, an ‘inertial mechanism’ is found for the smaller step diameter. However, for the larger step diameter, a ‘shock wave mechanism’ is identified due to the collapse of the vapor fragments at its exit.

References

- [1] Mauger C, Mèès L, Michard M, Azouzi A and Valette S 2012 *Experiments in Fluids* **53** 1895–1913
- [2] Iben U, Morozov A, Winklhofer E and Skoda R 2011 *WIMRC 3rd International Cavitation Forum 2011*, University of Warwick
- [3] Iben U, Morozov A, Winklhofer E and Wolf F 2011 *Experiments in Fluids* **50** 597–611
- [4] Stanley C, Barber T, Milton B and Rosengarten G 2011 *Experiments in Fluids* **51** 1189–1200
- [5] Duke D, Kastengren A, Tilocco F Z and Powell C 2013 *25th Annual Conference on Liquid Atomization and Spray Systems, ILASS-Americas, Pittsburgh, PA, May* pp 5–8
- [6] Schmidt S J, Sezal I H, Schnerr G H and Thalhamer M 2008 *46th AIAA Aerospace Sciences Meeting and Exhibit* pp 7–10
- [7] Chorażewski M, Dergal F, Sawaya T, Mokbel I, Grolier J P E and Jose J 2013 *Fuel* **105** 440–450
- [8] Ndiaye E H I, Bazile J P, Nasri D, Boned C and Daridon J L 2012 *Fuel* **98** 288–294